

Role of Oxygen Fugacity on the Melting Properties of Enstatite Chondrites and Implications for Mercury's Magmatic Evolution.

R. Gwyn¹, T. McCombs¹, S. Lambart², K. Righter³, L. R. Nittler⁴, A. Boujibar¹. ¹Department of Geology, Department of Physics and Astronomy, AMSEC (Advanced Materials Science & Engineering Center), Western Washington University, Bellingham, WA 98229, ²Department of Geology and Geophysics, University of Utah, Salt Lake City, UT 84112, ³NASA Johnson Space Center, Houston, TX 77058, ⁴School of Earth and Space Exploration, Arizona State University, Tempe, AZ 85287

Introduction: Mercury, the innermost terrestrial planet, is the most reduced planet in our solar system. Insights from MESSENGER mission data revealed the presence of several distinct geochemical terranes, evidence of complex magmatic processes and collisional processes exposing subsurface materials [1-4]. Surface chemical analysis indicated elevated S (~2-3 wt%) and low FeO (~1.5 wt%) concentrations [1, 4, 5]. The high sulfur concentration indicates reduced conditions with an average of 5.4 log units below the Iron-Wüstite (IW) oxygen fugacity (fO_2) buffer (IW-5.4) [2]. Surface compositions also show a range in redox conditions during mantle melting and eruption, with inferred log fO_2 , ranging from IW-6.5 to IW-3.5 [6]. The effects of oxygen fugacity on magmatic differentiation are poorly constrained, despite their significance in our understanding of mantle-crust differentiation in the solar system.

Enstatite High-Fe (EH) chondrites are very reduced undifferentiated meteorites with elevated concentrations of Fe and volatiles like S, Cl, Na, and K as compared to other chondrites [7]. These characteristics suggest that EH chondrites are a potential analog for Mercury's building blocks. However, the comparison of Mercury's surface composition with melting products of EH chondrites is necessary to determine whether Mercury surface materials may be derived from EH chondrite-like materials. Here, we investigate the role of fO_2 on EH melting properties and its implications for Mercury's accretion and differentiation.

Methods: Thermodynamic modeling using pMELTS [8] is employed to derive melting properties of EH4 Indarch chondrites as a function of oxygen fugacity. The starting composition is that of the EH4 Indarch chondrite [9], modified to account for variations in oxygen fugacity. Since pMELTS modeling does not account for the presence of metallic phases, modeling was performed on the silicate fraction of the chondrites. Previous experimental studies have shown that as the fO_2 decreases, silicon becomes more metallic through the reaction: $SiO_2^{Silicate} = Si^{Metal} + O_2$. Hence, in a system where only redox conditions vary, as fO_2 increases the silicate fraction becomes enriched in SiO_2 ,

and the Mg/Si and Al/Si ratios decrease, while the metallic fraction gets enriched in Si (see red triangles in Fig. 1). Using pMELTS, we modeled batch melting at 1 GPa for these different starting compositions and investigated liquidus temperatures, phase relations and melt compositions.

Results and Discussion: The pMELTS thermodynamic results suggest that increased Si_{metal} changes the melting properties substantially. Liquidus temperature increases by ~80°C from 1513°C to 1593°C when Si_{metal} increases from 1 to 18 wt%. Converting the Si_{metal} to SiO_2 ratio in our models leads to substantial variations in Mg/Si and Al/Si ratios, contingent on the initial Si_{metal} and the degree of melting within the system.

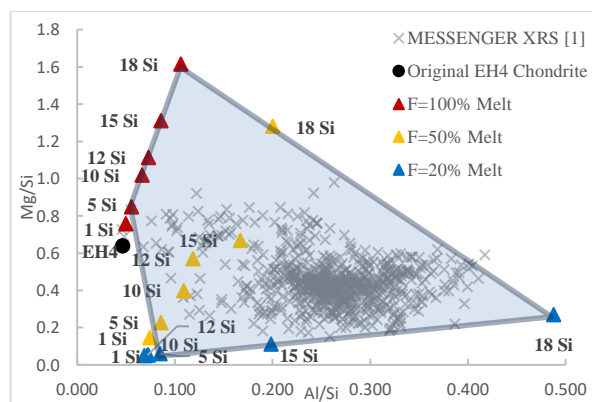


Figure 1: Silicate melt compositions derived from pMELTS modeling (triangles) compared with Mercury's surface composition from MESSENGER XRS measurements (grey crosses) [1]. F represents the melt fraction for each model. Starting compositions (red triangles) are calculated by reducing a fraction of SiO_2 into metallic Si, such that the metallic fraction of the modified chondrite has 1 to 18 wt% Si metal (1 Si to 18 Si, respectively). The shaded polygon represents the broad compositional variability of melts produced by batch melting at 1 GPa and the Indarch EH4 is shown with the black circle [7, 9].

Starting compositions or melts derived from complete melting (F=100% in Fig. 1), Mg/Si increases significantly from 0.758 to 1.614 for 1 wt% and 18 wt% Si_{metal} , respectively, while Al/Si ratios show a moderate

increase from 0.049 to 0.106. In contrast, at lower melt fractions ($F=20\%$), Al/Si ratios exhibit considerable variability, ranging from 0.072 to 0.487 across 1 to 18 wt% Si_{metal} . The shaded polygon in Fig. 1 shows the broad variability of melt compositions across all melt fractions and $f\text{O}_2$ conditions investigated.

Given the heterogeneous mantle $f\text{O}_2$ implied by the S content observed on Mercury's surface [6], our results suggest significant variability in magmatic compositions. A heterogeneous $f\text{O}_2$ within Mercury's mantle is expected to yield magma reservoirs with a wide range of compositions. In addition, one striking result is the overlap (Fig. 1) between the broad range of melt chemical compositions shown with the shaded polygon and Mercury's surface composition shown with crosses (MESSENGER's XRS data [1]). Therefore, the heterogeneous chemical composition of Mercury's surface could be the result of variations in oxygen fugacity in Mercury's mantle. Particularly, highly reduced compositions and low degrees of melting can produce high Al/Si ratios, while higher degrees of melting and more oxidized compositions can produce low Al/Si ratios.

Most Mercury compositions overlap with models where the degree of melting is lower than 50% and the metal fraction contains 12 to 18 wt% Si. This result adds a new constraint on Mercury's core composition for a model of Mercury formed with EH chondrites. Since metals incorporate Si at low $f\text{O}_2$, this, it confirms the reducing nature of the planet interior suggested by its surface iron oxide and sulfur concentrations.

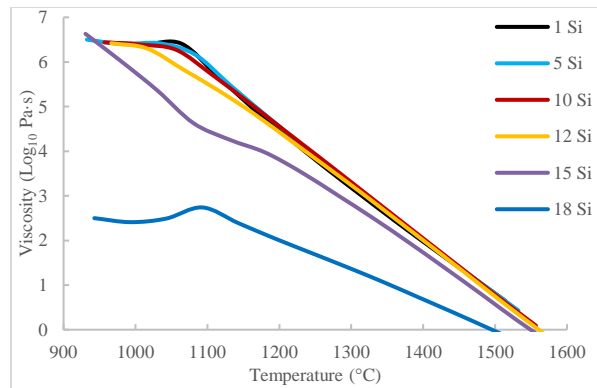


Figure 2. Viscosity of silicate melts derived from pMELTS as a function of temperature, for each starting composition at 1 GPa.

In addition to the compositional changes of melts resulting from varying $f\text{O}_2$, their physical properties are also affected. The viscosity of the silicate melts (Fig. 2) experiences a substantial decrease by several orders of magnitude as Si_{metal} increases from 12 to 18 wt%. This effect is dramatic at low temperature, where viscosity

drops from $10^{6.5}$ (like dacites) to $10^{2.5}$ Pa·s (like basalts or andesites) at 1000 °C. This phenomenon is predominately attributed to the reduction of SiO_2 content in the silicate melt at low oxygen fugacity, yielding less polymerized melts. While the variation of temperature and composition is known to significantly affect magma viscosity, changing $f\text{O}_2$ exacerbates this contrast in rheology. These results are likely to have important implications for eruptive processes, Mercury mantle dynamics, as well as convection and mixing of the crystallizing magma ocean [10].

Conclusion: Oxygen fugacity plays a pivotal role in the formation and differentiation of planets within our solar system, influencing both the composition and viscosity of silicate melts. Our pMELTS modeling underscores how the compositionally diverse surface of Mercury can be explained by variations in $f\text{O}_2$ of Mercury's mantle. Such variations can result from the preservations of heterogeneities if the magma ocean is not well mixed during its crystallization. It can also result from later chemical changes due to the fractionation of sulfides [11] or graphite-induced smelting [12].

References: [1] Weider et al. (2015) EPSL, 416, 109-120. [2] Namur et al. (2016) EPSL, 439, 117-128. [3] Nittler et al. (2020) Icarus, 345, 113716. [4] Wang et al. (2020) JGR Planets, 127, e2022JE007218. [5] Weider et al. (2012) JGR, 117, E00L05. [6] Namur et al. (2016) EPSL, 448, 102-114. [7] Wiik (1956) GCA, 9, 279-289. [8] Ghiorso et al. (2002) G³, 3, 5. [9] Berthet et al. (2009) GCA, 73, 6402-6420. [10] Mouser et al. (2021) JGR Planets, 126, e2021JE006946. [11] Boukaré et al. (2019) JGR Planets, 121, 3354-3372. [12] McCubbin et al. (2017) JGR Planets, 122, 2053-2076.